



Synthesis and Characterization of a Thin-Film Composite Nanofiltration Membrane Based on Polyamide-Cellulose Acetate: Application for Water Purification

Ibtissem Ounif^{1,2} · Youssef Guesmi^{1,2} · Claudia Ursino³ · Roberto Castro-Muñoz⁴ · Hassen Agougui^{5,6} · Mahjoub Jabli^{7,8} · Amor Hafiane¹ · Alberto Figoli³ · Ezzedin Ferjani⁹

Accepted: 3 July 2021 / Published online: 9 July 2021

© The Author(s), under exclusive licence to Springer Science+Business Media, LLC, part of Springer Nature 2021

Abstract

Membrane separation has been widely used for various applications including microfiltration (MF), ultrafiltration (UF), and nanofiltration (NF) processes in the fields of biomedicine, food, and water purification. In this work, a facile synthesis of new polyamide thin-film composite nanofiltration membranes (NF-TFC) for water purification was described. The polyamide thin film was deposited over a synthetic cellulose acetate (CA) support by interfacial polymerization method. 1,3 cyclohexane bis (methylamine) (CHMA) and trimesoyl chloride (TMC) were used as monomers. The membranes were characterized using Scanning Electron Microscopy (SEM), Fourier Transform Infrared spectroscopy (FT-IR), water uptake, porosity, contact angle, water permeability and rejection towards specific salt and dye molecules. The effect of the variation of the CHMA concentration (0.2–2 wt.%) on the morphology, porosity, water permeation and rejection properties of the prepared membranes was studied. SEM results displayed the growth of the membrane thickness when the CHMA concentration increased from 0.2 to 2 wt.%. The strong adhesion between the cellulose acetate substrate and the polyamide layer explained by the formation of the polyamide film in the substrate surface and inside the pores. The water permeability varied from 36.02 to 17.09 L h⁻¹ m⁻² bar⁻¹. The salt rejection of Na₂SO₄ and NaCl increased from 9 to 68% and from 38.41% to 89.4%, respectively, when the CHMA concentration was changed from 0.2 to 2 wt.%. The prepared membranes were further applied successfully for the removal of malachite green and congo red. The results indicated that the maximum rejection reached 89% and 85% for malachite green and congo red, respectively.

Keywords Polyamide NF membrane · Thin-film · Interfacial polymerization · Malachite green · Congo red

✉ Hassen Agougui
hassenagougui@yahoo.fr

✉ Mahjoub Jabli
mahjoub_jabli@yahoo.fr; m.jabli@mu.edu.sa

¹ Laboratory of water, membrane and environmental biotechnology, Centre of Research and Water Technologies, Technopark of Borj-Cedria, BP 273, 8020 Soliman, Tunisia

² Faculty of Sciences of Tunis, University of Tunis - El Manar, 20 Toleda street, Tunis, Tunisia

³ Institute on Membrane Technology (ITM-CNR), Via P. Bucci 17 c, 87036 Rende, CS, Italy

⁴ Tecnológico de Monterrey, Campus Toluca, Avenida Eduardo Monroy Cárdenas 2000 San Antonio Buenavista, 50110 Toluca de Lerdo, Mexico

⁵ Laboratory of Physical-chemistry of Materials, Faculty of Sciences of Monastir, 5019 Monastir, Tunisia

⁶ Faculty of Sciences of Gafsa, University of Gafsa, University Campus, Zarroug, 2112 Gafsa, Tunisia

⁷ Department of Chemistry, College of Science Al-zulfi, Majmaah University, Al-Majmaah 11952, Saudi Arabia

⁸ Textile Materials and Processes Research Unit, Tunisia National Engineering School of Monastir, University of Monastir, Monastir, Tunisia

⁹ Higher Institute of Science and Technology of Environment of Borj-Cedria, Bp 2050, Borj-Cedria, Tunisia

Introduction

The development of the industrial sector and the increasing demand for textiles has conducted to the use of the synthetic organic dyes in a wide range of textile fibers, such as polyester, polyamide, cotton, etc. Nowadays, textile dyeing represents one of the highest water-consuming industries, and it generates large quantities of carcinogenic organic dyes and inorganic salts, which have a negative impact on the aquatic environment and human health [1, 2]. Therefore, several methods have been used to remove dyes from contaminated water such as adsorption [3, 4], electrochemical [5], advanced oxidation processes including chemical oxidation and catalytic degradation [6, 7], etc. However, the above-mentioned processes have been reported to be quite costly and/or causing additional toxic sludge or even not practical for large-scale application [6–8].

Due to several advantageous features such as the easy scale-up and the relatively low energy consumption, NF has been emerged as an excellent candidate in a wide variety of separation applications, particularly in the pharmaceutical, textile, and agro-food sectors [9–15]. Commonly, NF selectively rejects molecules having a size ranging between 0.5 and 2 nm such as multivalent salts, dyes, and organic matters with molecular weight of 200–1000 Da [16–19]. Several techniques were reported in the literature for the preparation of nanofiltration membranes such as polymerization plasma preparation [20], layer-by-layer [21], UV grafting [22, 23], interfacial polymerization [24, 25], among others. In particular, the interfacial polymerization, reported by Cadotte in the early 1980s, was considered the most widely used technique since thin-film composite (TFC) membranes largely dominated the polymeric NF membranes market [26]. A TFC membrane consists of at least two distinct layers; a porous substrate conferring a sufficient water flux and a top active layer that controls the whole membrane selectivity [25–27]. To date, it is likely that the most popular TFC membranes are based on polyamide (PA) selective layer. The PA layer is formed on the porous substrate as a result of a reaction occurring at the interface between an organic solution containing chloride acid-type compounds and an aqueous solution containing an aliphatic/aromatic diamine [25]. Despite TFC membranes have been well received in the industry, membrane scientists still well interested in developing TFC membranes to break the typical trade-off relationship between permeability and selectivity. For instance, Langming et al. [28] have been incorporated the cellulose nanocrystals (CNCs) into PA layer through interfacial polymerization to improve the physicochemical properties of TFC membranes (CNC-TFC). The resulted TFC membrane showed

a great rejection performance for divalent salts (ca. 98%) and dyes (over 99%). More recently, Meng et al. [29] used sodium alginate and polyvinylidene fluoride (PVDF) substrate to prepare PVDF-CaAlg nanofiltration membranes with dual thin-film-composite. The results showed that the prepared membranes exhibited superior surface hydrophilicity which improved the pure water flux and the removal rate for congo red reached 98.4%. Zirehpour et al. [30] developed thin-film PA layer modified by metal-organic framework (MOF) nanocrystals over PES substrate. The results showed that the modified membrane with 0.04% MOF increased the pure water permeability without affecting the selectivity. The enhancement of the membrane properties was explained by the better compatibility between the organic linker of the MOF and the organic polymer through hydrogen bonds and covalent bonds formed between the two phases.

The aforementioned examples illustrate that the modification of the active layer of the TFC membrane can effectively improve their performance. In itself, the active layer in TFC membranes was strongly affected by the type of the monomer used in the IP process. In this respect, several monomers were tested, including piperazine (PIP) [31], m-phenylenediamine (MPD) [32], and bisphenol A (BPA) [23] in the aqueous phase, and trimesoyl chloride (TMC) [33, 34] and terephthaloyl chloride (TPC) [35] in the organic phase.

Even though the trend of research involved in the development of TFC membranes significantly increased in the last decade, many efforts are still needed to produce membranes with the desired properties. This calls for testing new substrates other than the conventional ones and the use of new precursors for developing the PA layer [36]. Based on the available literature, CA as a substrate for TFC membrane and CHMA as a monomer for PA preparation had not been widely used in the preparation of PA TFC [37]. Herein, our current work was devoted to the preparation of a new PA TFC nanofiltration membranes by interfacial polymerization. The cellulose acetate substrate (CA UF), previously investigated as ultrafiltration membrane in our previous study [38] and the monomers couple of CHMA and TMC, respectively in the aqueous phase and in the organic phase were used to produce new TFC membranes. The effect of CHMA concentration during the preparation procedure was investigated. The resulting membranes were characterized using FTIR, SEM, water uptake, porosity, and contact angle. The water uptake and the contact angle were measured as a function of CHMA concentration. The membrane performance was evaluated by measuring the pure water permeability and salt rejection (NaCl and Na₂SO₄). The prepared membranes were further checked for the removal of Congo red and malachite green.

Experimental

Reagents and Chemicals

Cellulose acetate (MW = 30,000 g mol⁻¹, 39.8 wt.% acetyl), acetone, formamide (purity ≥ 99.5%), hexane (purity ≥ 95%), 1,3-cyclohexanbis(methylamine) (Molecular weight = 142.24 g mol⁻¹, purity ≥ 98%), trimesoyl chloride (Molecular weight = 265.48 g mol⁻¹, purity ≥ 98%), Congo red (C₃₂H₂₂N₆Na₂O₆S₂, Molecular weight = 696.66 g mol⁻¹, purity ≥ 85%) and malachite green (C₅₂H₅₄N₄O₁₂, Molecular weight = 927.02 g mol⁻¹, purity ≥ 90%), NaCl, Na₂SO₄ were purchased from Sigma Aldrich. Distilled water was used for rinsing the membrane samples and to prepare the aqueous solutions of salts and dyes. The chemical structures of the monomers and the dyes were shown in Fig. 1, while some properties of the studied dyes were summarized Table 1.

Microporous Cellulose Acetate Support Preparation

The microporous substrate of the TFC membrane was prepared from CA polymer, largely used for polymeric membrane fabrication [39–41]. Polymeric solution was prepared by dissolving CA (15 wt.%) in acetone-formamide (2:1; v/v) solution at 25 °C. The dope solution was stirred for 24 h until the polymer was completely dissolved. Later, the dope solution was casted onto a glass plate with a casting knife set at 200 μm. The glass plate was then immersed for 1 h in a water coagulation bath at 4 °C without further evaporation time. Finally, to remove the remaining solvent, the

Table 1 Properties of Congo red and malachite green

Dye	Formula	Molecular weight (g mol ⁻¹)	λ _{max} (nm)
Congo red	C ₃₂ H ₂₂ N ₆ Na ₂ O ₆ S ₂	696.6	498
Malachite green	C ₅₂ H ₅₄ N ₄ O ₁₂	364.9	618

resulting membrane was immersed in a bath of distilled water at 60 °C.

Preparation of Thin-Film NF Composite Membranes

The TFC membranes were prepared by IP technique using microporous synthetic cellulose acetate ultrafiltration membranes as support (CA UF). The support membranes were taped onto a glass plate leaving the topmost surface available for reaction. Initially the membranes were immersed in a several concentrations of CHMA aqueous solution (0.2, 0.5, 1, 2 wt.%) for 2 min at room temperature. The pre-soaked membranes were later taken out from the aqueous solution, and vertically positioned for 1 min to drain the excess monomer on the membranes surface. Then, all the membranes were dipped for 1 min in the organic phase of hexane and the monomer TMC (0.1 wt.%), until reaching the complete IP. The reaction of the monomers CHMA and TMC occurs at the membrane surface and thus producing a PA layer. The typical polymerization reaction between such reactants is depicted in Fig. 2.

Fig. 1 Chemical structure of the studied dyes and the used monomers: **a** congo red, **b** malachite green, **c** 1,3-Cyclohexanbis(methylamine), and **d** Trimesoyl chloride

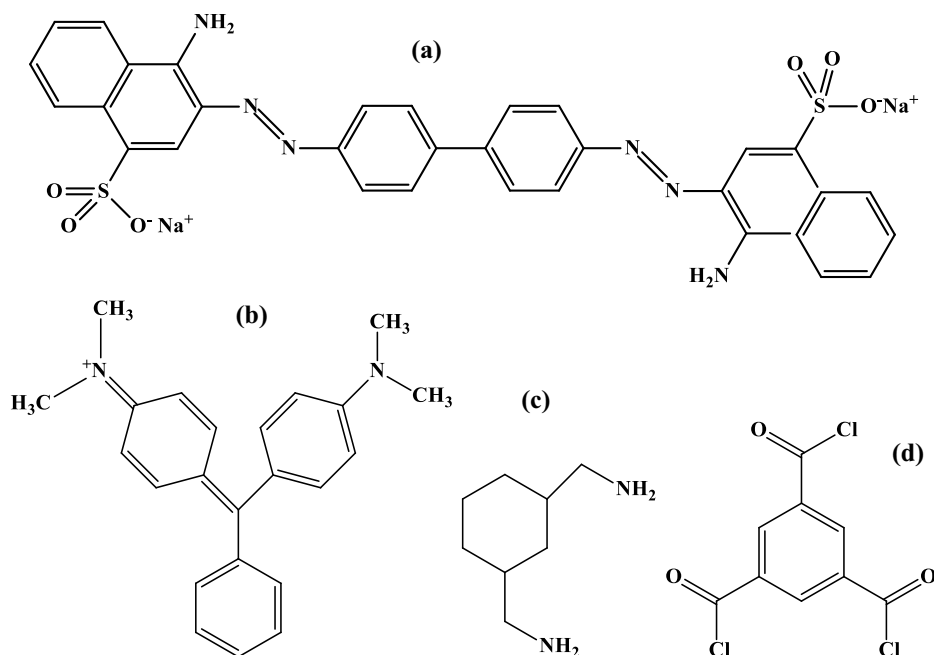


Fig. 2 The polymerization reaction between CHMA and TMC

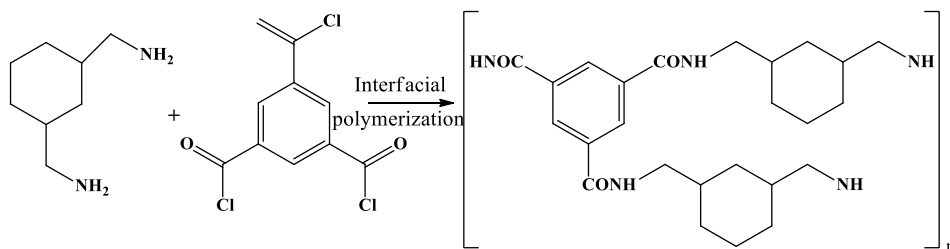


Table 2 Summary of TFC membranes prepared in this study

Membranes	CHMA (wt.%)
CA UF	0
TFC-0.2	0.2
TFC-0.5	0.5
TFC-1	1
TFC-2	2

Finally, the membranes were dried in air for 30 min to evaporate the organic solvent. The resulting TFC membranes were stored in pure water overnight before characterization tests. All TFC membranes prepared in this work were listed in Table 2.

Characterization Instruments and Methods

The effect of CHMA concentration on the surface and cross-section morphology of the membranes was studied using a Scanning Electron Microscopy (Zeiss EVO MA 100, Assing, Italy). The membrane samples were spattered with gold before observation. The chemical structures of the substrate layer (CA UF) and the TFC membrane (TFC-2) were investigated using Fourier transform infrared spectroscopy instrument with IR (IRAffinity-1S, Tunisia). The measurements were performed in the wavenumber range of 450–4000 cm^{-1} .

The surface wettability of the membranes was evaluated using an Attension Theta optical tension-meter (Biolin Scientific, Tunisia). The measurements were performed using ultra-pure water drop (5 μL). The measurements were performed at least five times for each sample and the average was noted-down. The porosity ($\epsilon\%$), defined as the ratio between the volume of voids in the membrane and the whole membrane volume, was determined using gravimetric method [42]. The dry membrane was weighed and then immersed in kerosene for 24 h. Then, the excess of kerosene was eliminated, and the membrane was weighed once again. The porosity was determined using Eq. 1:

$$\epsilon(\%) = \left\{ \frac{(W_w - W_d)/\rho_k}{(W_w - W_d)/\rho_k + \frac{W_d}{\rho_p}} \right\} \quad (1)$$

where ϵ is the membrane porosity (%), W_w and W_d are the wet and dry weight of the membrane, respectively, ρ_p is the polymer density (1.28 g cm^{-3}), ρ_k is the density of kerosene (0.82 g cm^{-3}).

The water uptake of the prepared membranes was performed using Eq. 2 [43]:

$$\text{Water uptake} = \left(\frac{(M_w - M_d)}{M_w} \right) \times 100 \quad (2)$$

where M_w and M_d are the wet and dry weight of the membrane sample, respectively.

Pure Water Flux and Rejection

Distilled water was used to perform membrane permeability to pure water. The membrane performances were evaluated using sodium salts (NaCl , Na_2SO_4) aqueous solutions with a concentration of 20 mg L^{-1} and dyes (Congo red and malachite green) aqueous solutions with concentrations of 10, 20, 50, and 100 mg L^{-1} . In all cases, the membrane performance was determined using stainless steel cell (Millipore) with a total volume of 350 mL, and effective membrane area of 38.54 cm^2 . Before measurements, the membrane was compacted for 1 h at 16 bar. The pure water flux, salt and dyes rejection tests were determined at a pressure of 9 bar. The effect of pH variation on dyes retention was investigated in the range of 2–12 by either adding solution of NaOH (0.1 M) or HCl (0.1 M). The permeate flux was measured as water volume permeating per unit area membrane at specific time:

$$J_V = \frac{v}{A\Delta t} \quad (3)$$

where J_V is the permeate flux ($\text{L m}^{-2} \text{h}^{-1}$), v is the volume of permeate (L), A is the membrane area (m^2) and Δt is the operating time (h).

The retention rate of salts and dyes was calculated as follows:

$$R(\%) = \left(1 - \frac{C_p}{C_f}\right) \times 100 \quad (4)$$

where, C_f and C_p are the concentrations of feed and permeate solutions, respectively. The measurement of the dye concentration before and after filtration was performed using an UV Perkin–Elmer Lambda 25 spectrophotometer.

Results and Discussion

SEM Morphology Characterization

Figure 3 showed the morphology (cross section, top and bottom side) of the CA UF membrane used as substrate, as well as TFC membranes using the lowest (0.2 wt.%) and highest (2 wt.%) content of CHMA (TFC-0.2 and TFC-2, respectively). The CA UF membrane showed the typical asymmetric structure of the phase inversion technique, which has been also reported in the literature

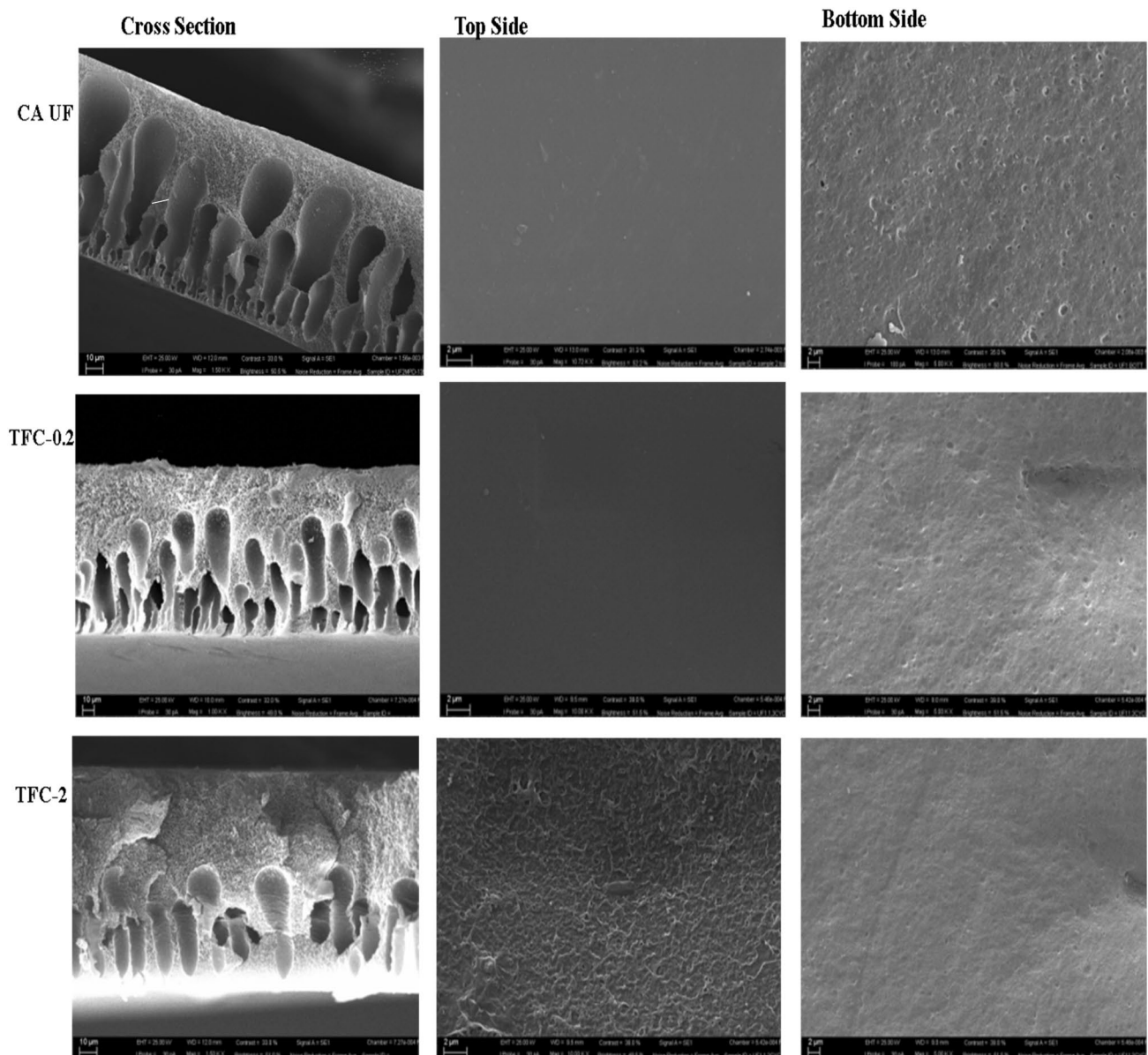


Fig. 3 SEM images of CA UF support, TFC-0.2 and TFC-2 composite polyamide membranes [cross section ($\times 1500$ K), top side ($\times 10,000$ K) and bottom side surface ($\times 5000$ K)]

[44–47]. Moreover, CA UF exhibited a relatively smooth and defect-free surface (top side image), with some pores that appear, especially, on the bottom side. Whereas the cross-section image of the substrate showed large pores with a finger-like structure.

After the PA layer being deposited over the CA UF substrate, the surfaces of the TFC membranes (TFC-0.2 and TFC-2) became denser and turned to a rougher structure (top side images). In particular, the top side image of TFC-2 showed a rougher surface with nodular morphology generated by the “ridge and valley” structure, which is the common structure of polyamide films [48]. The roughness structure could be attributed to the stress during the IP reaction and swelling in the drying process. Firstly, the support saturated with CHMA was in contact with TMC. Herein, the amine monomer, transported by diffusion to the interface by hexane and later reacts with the TMC. While when the TFC was dried in the air, the solvent evaporated from the membrane top surface, resulting in an uneven-type surface.

The cross-section images of the TFC membranes showed that when CHMA concentration increased the selective layer thickness grows and the size of the pores becomes tighter and transformed to the dead-end form compared to the CA UF substrate. In that, when the CHMA concentration was increased from 0.2 to 2 wt.%, more monomer species were deposited on the surface of the membranes. Hence, during IP, more CHMA can react with TMC and subsequently increase the thickness of the membranes, which expected also to improve the selectivity during the nanofiltration studies.

Eventually, the images of the bottom side show that the pores which appeared in the CA UF substrate gradually disappeared with increasing the CHMA concentration. This finding suggests that the PA layer was formed in the pores

in addition to the substrate surface, conferring more stability in case of high pressure running.

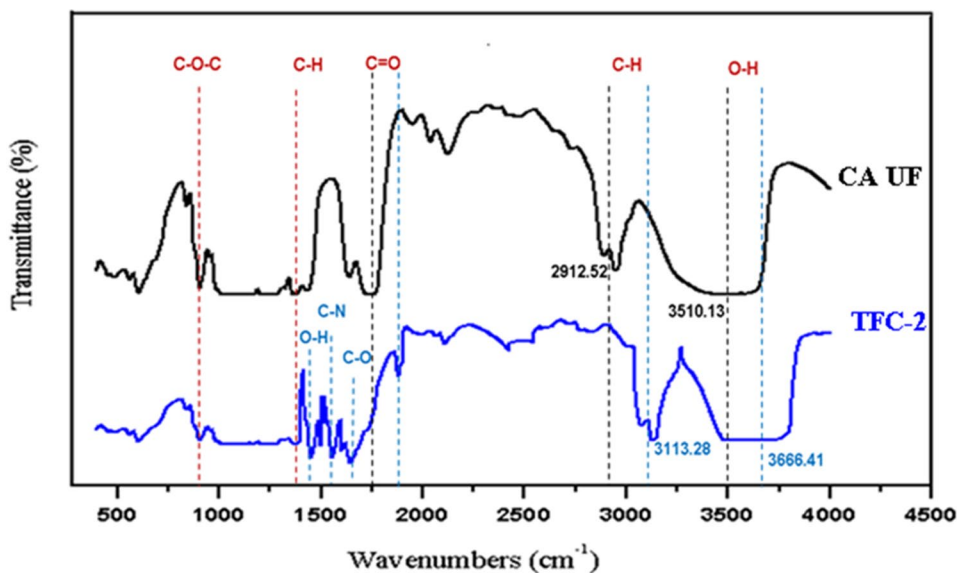
FT-IR Spectroscopy Investigation

Figure 4 reported the FT-IR spectra of the CA UF substrate and TFC membranes. The FT-IR spectrum of the support membrane displayed the characteristic bands of the CA such as O–H (around 3510.13 cm^{-1}), C–H (around 2912.52 cm^{-1}), C=O (1750 cm^{-1}), C–H (1372 cm^{-1}) of $-\text{CH}_3$, and C–O–C (917 cm^{-1}) of ether from the glycosidic linkage [49, 50]. Compared with the CA UF substrate, new absorption peaks characteristics of polyamide appeared in the range of $1400\text{--}1700\text{ cm}^{-1}$ in the FT-IR spectrum of the TFC-2 membrane which confirms the success of the interfacial polymerization. The peak appearing at 1453 cm^{-1} is ascribed to the O–H deformation of carboxylic acid. The strong absorption band registered at 1559 cm^{-1} was assigned to the amide group C–N in-plane bending [51]. While the absorption band seen at 1642 cm^{-1} was attributed to the C–O groups characteristic of the amide group [51]. Moreover, the characteristic bands of the CA UF membrane showed a slight shift to higher wavenumbers values in the FT-IR spectrum of the TFC-2 as mentioned in Fig. 4. In particular, the bands of C=O, C–H, and O–H were moved to around 1895.63 ; 3113.28 ; and 3666.41 cm^{-1} , respectively.

Contact Angle Measurement

The wettability of membranes surface was evaluated by means of water contact angle measurements. Figure 5 shows the average water contact angle values for the TFC membranes as a function of the CHMA content. All the membranes showed contact angles below 90° , which confirms

Fig. 4 FT-IR spectra of CA UF support and thin-film composite TFC-2



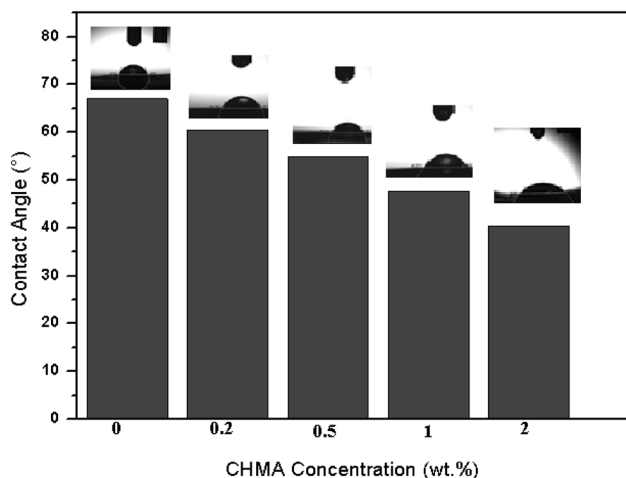


Fig. 5 Change of the contact angle of the TFC membranes as a function of CHMA concentration (0-0.2-0.5-1-2)

their hydrophilic nature. The contact angle decreased from 65° to 40° when CHMA concentration increased from 0 to 2 wt.% and membranes hydrophilicity followed the order of $UF < TFC-0.2 < TFC-0.5 < TFC-1 < TFC-2$.

In fact, the increase of the CHMA concentration provides more hydrophilic polar amide functional groups on the membrane surface and consequently an improvement of the hydrophilic behavior [52]. Moreover, the improvement of the rugosity after depositing the thin film layer could be another reason for the decrease in contact angle values.

The hydrophilic behavior makes favors the transfer of water molecules across the membrane rather than the other pollutants giving more selectivity during filtration [53].

Water Uptake Property

Figure 6 displayed the water uptake of the prepared membranes at different CHMA concentrations. It was found that the water content decreased from about 76% to 50% when the CHMA concentration increased from 0 to 2 wt.%. Generally, the increase of the membrane hydrophilicity creates new stream ways for water transport, improving water uptake [54]. However, in this study, the hydrophilicity behavior surges together with the decrease in water uptake. This result means that the water uptake was mainly related to the other properties of the upper layer including the crosslinking degree and the pore size of the formed PA. In particular, the increase of the polyamide thickness explains the strong polymer interactions. Hence, the increase of the cross-linkage could restrict the mobility of PA chains, rendering a weak water uptake. In addition, the decrease in water uptake values could be justified by the decrease of porosity observed by SEM images, which does not provide free spaces for

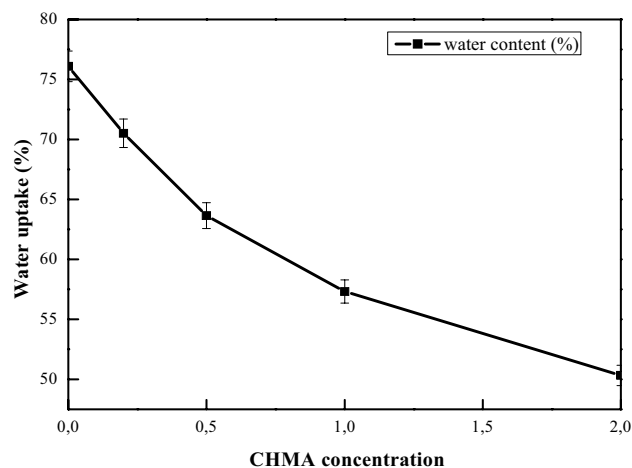


Fig. 6 Water uptake of the TFC membranes as a function of the CHMA concentration (0-0.2-0.5-1-2)

water hosting. In fact, such results are in agreement with the reduction of porosity as a function of CHMA content.

Permeability and Porosity Characteristics

Figure 7 shows the influence of CHMA concentration on the porosity and the pure water permeability of the CA UF and TFC membranes. The results clearly show that water permeability and porosity were strongly affected by the increase of the CHMA concentration. The porosity decreased from 70 to 40% when the CHMA concentration increased from 0 to 2 wt.%. Correspondingly, water permeability was reduced drastically from 36 to $17 \text{ L h}^{-1} \text{ m}^{-2} \text{ bar}^{-1}$ for the same CHMA concentration variation. These results suggest the formation of denser and lesser permeable PA layers at higher CHMA

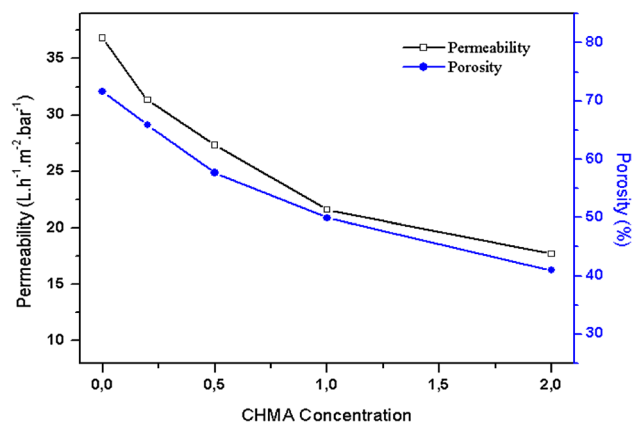


Fig. 7 Pure water permeation and porosity as a function of the CHMA concentration (0-0.2-0.5-1-2) (amine=2%; curing temperature = 25°C ; curing time = 2 min)

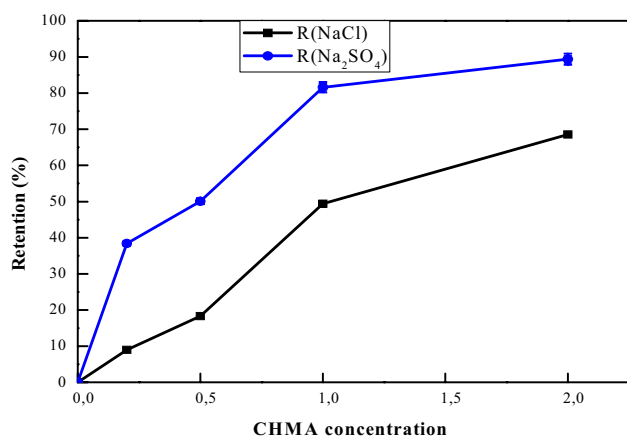


Fig. 8 Salts retention in TFC membranes as a function of CHMA concentration (0-0.2-0.5-1-2) (TMC=1%; curing temperature=25 °C; curing time=1 min)

concentrations. The decrease of membrane permeability is due to the reduction of porosity and to the additional permeation resistance generated from the thick and compact PA layer. A similar result was also found by other researchers [55, 56]

Effect of CHMA Concentration on the Salt Retention Performances

Figure 8 gave the rejection ability towards salt molecules as a function of CHMA concentration. The results indicated that the prepared membranes showed an increase in salt retention when the CHMA concentration increased from 0 to 2 wt.%. Firstly, at low monomer concentration 0.2 wt.%, the retention was about 9% and 38% for NaCl and Na₂SO₄, respectively. Therefore, at this concentration, the CHMA concentration was not enough for a complete polymerization reaction [57]. On the contrary, the increase in CHMA concentration displayed a dependent increase towards NaCl and Na₂SO₄ rejection. Herein, the highest retentions rates were found at the highest CHMA concentration (i.e., 2 wt.%), where the salt rejection was about 68% and 89% for NaCl and Na₂SO₄, respectively. It is worth to mention that CHMA concentration (i.e., monomer concentration) plays a crucial role in the preparation of the membranes by interfacial polymerization technique. Precisely, increased CHMA concentration tends to boost the crosslinking degree, which was likely responsible for the simultaneous decrease in water permeability and increase in salt rejection. In fact, the typical trade-off relationship between permeability and selectivity of the TFC membranes was widely mentioned in previous studies with other monomers [53, 58]. On the whole, the TFC-2 membrane exhibits a good compromise between permeability and salts rejection.

Effect of CHMA Concentration on the Dyes Removal

TFC membranes performance were also evaluated for dyes removal, using Congo red and malachite green and the results were presented in Fig. 9. In principle, all TFC nanofiltration membranes showed higher dye rejection compared to the CA UF substrate. Clearly, the rejection rate was strongly affected by the monomer concentration. In other words, the dyes rejection increased when the CHMA concentration increased. For instance, the raising of the CHMA concentration from 0 to 2 wt.% increased the retention rate, from 12 to 89% for malachite green and from 10 to 85% for Congo red. It has been noticed that the rejection was slightly better for malachite green. In theory, the molecular weights of such compounds are different, e.g., 364.9 and 696.7 g mol⁻¹ for malachite green and Congo red, respectively; and therefore, it could be expected to have a higher retention rate towards Congo red. However, as these pressure-driven processes are based on molecular sieving effect, their molecular size is crucial for their rejection which are 0.7 and 0.8 nm for Congo red and malachite green, respectively. From these results, it may conclude that the dyes retention by the thin-film composite nanofiltration membrane depended on the dye molecular size [11, 59].

Additionally, the TFC-2 membrane was used to explore the dye retention as a function of the dye concentration and the results were illustrated in Fig. 10. An increase in retention for both types of dye was found when the dye concentration increased. For example, the highest retentions rates (at 100 mg mol⁻¹) were about 89% and 76% for malachite green and Congo red, respectively. While the lowest retention rates (around 50% and 40% for malachite green and Congo red, respectively) were found at the lowest dye concentration (at 10 mg L⁻¹). Typically, when the concentrations of the dyes are higher, membranes are able to absorb molecules

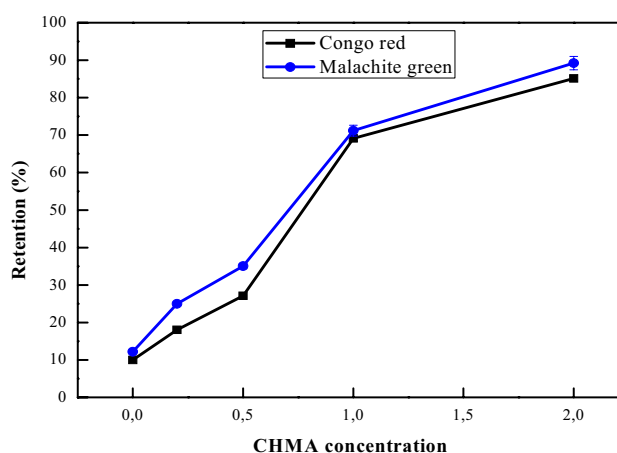


Fig. 9 Dye retention in TFC membranes as a function of CHMA concentration (0-0.2-0.5-1-2) (pH=6.8, T=25 °C, pressure=9 bar)

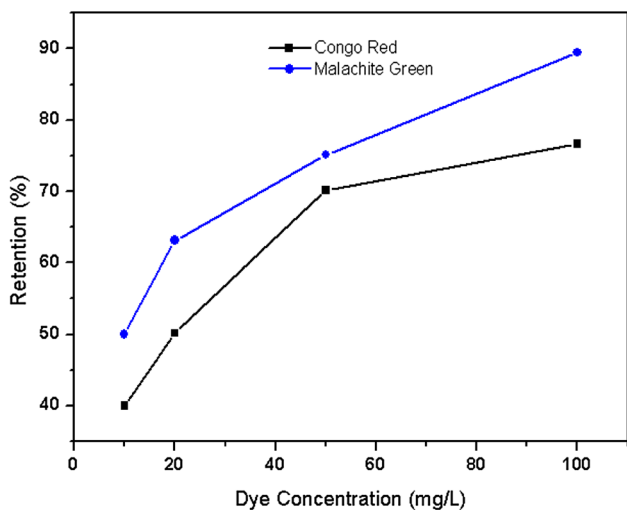


Fig. 10 Dye removal of TFC membranes as a function of the dye concentration in the feed (pH=6.8, T=25 °C, pressure=9 bar)

easily. On the other hand, increased concentration promotes the formation of another filter barrier through the gel layer formed by the accumulated dye molecules. The thickness of this layer increases by increasing the concentration of the dye, which enhances the retention rate. Compared to other published studies, the results obtained in this work indicated that the synthesized samples, notably TFC-2, are effective and could remove organic pollutants from water efficiently (Table 3).

Further analysis of TFC-2 performances on the removal of Congo red and malachite green was performed using the effect of pH variation and the results were reported in Fig. 11. The concentration of the dyes, pressure, and temperature were maintained constant. The data clearly indicate that there are significant differences in dye removal rates and their changing behaviors with the variation of the pH of feed dye solutions. Inversely to the rejection of Congo red which increased with the increase of pH, the maximum rejection of malachite green was achieved at lower pH values. This result suggests that the membrane separation properties are

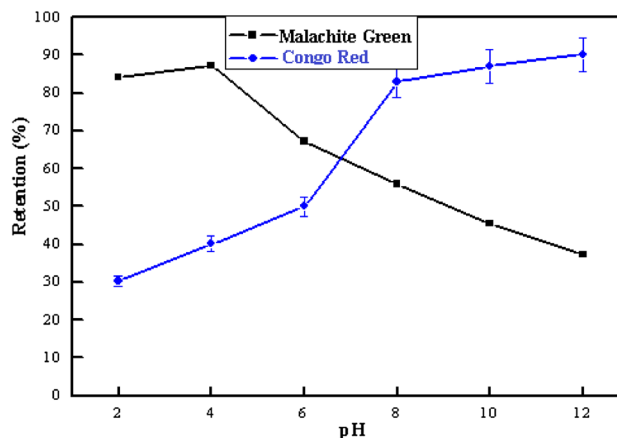


Fig. 11 Dye retention in TFC membranes as a function of pH (2–12) (concentration=10 mg, T=25 °C, P=9 bar)

determined mainly by electrostatic repulsion known as the Donnan exclusion effect [62]. The polyamide membranes in the acidic medium are positively charged owing to the strong protonation of NH₃. Thus, the positively charged membrane rejected the cationic dye (malachite green). While, when the membrane turned to the negative charge in the alkaline medium, the anionic dye (Congo red) reached a maximum rejection rate through the Donnan exclusion. Herein, this approach can give us an insight that when the dye concentration is low, the change of pH could be a good alternative for enhanced retention. It is clear that the congo red can be better retained (e.g., over 80%) at pH values over 8, while the malachite green reaches its better retention (e.g., >68%) at low pH values (below 6).

Conclusion

In this study, a series of polyamide TFC membranes were successfully prepared using the interfacial polymerization method. The UF CA membrane was used as substrates. The monomers of CHMA and TMC were used,

Table 3 A comparative study between some published membranes and the synthesized CA UF and TFC-2 membranes in this study

Membrane	Dye	Dye concentration (ppm)	Rejection (%)	Permeability (L m ⁻² h ⁻¹ bar ⁻¹)	References
PVDF-CaAlg-10	Congo red	20	98.3	32.5	[29]
TFC-control-M	Congo red	–	97.4	12.3	[60]
CNC-TFC-M6	Congo red	–	99.83	20.3	
PES18P4CWNT0.1	Malachite green	30	98.7	5.3	[61]
CA UF	Malachite green	100	12	36	This study
	Congo red	100	10		
TFC-2	Malachite green	100	89	17	This study
	Congo red	100	85		

respectively, in the aqueous phase and organic phase to produce the PA layer over the CA UF substrate. The effect of CHMA concentration (0, 0.2, 0.5, 1, and 2 wt.%) on the physicochemical properties of the prepared membranes was investigated using SEM, FT-IR, water uptake, porosity, contact angle, water permeability, and rejection rate of specific salt and dye molecules. SEM analyses showed the increase of the rugosity and the thickness of the membranes by increasing CHMA concentration. The TFC-2 membrane exhibited the common morphology of the polyamide membranes distinguished by the “ridge and valley” structure. FT-IR results showed new absorption bands characteristic of polyamide which confirm the success of the interfacial polymerization. The increase of the CHMA concentration enhanced the hydrophilicity and declined the porosity and permeability of the membrane; e.g., water permeability changed from 36.02 for CA UF membrane to 17.09 L h⁻¹ m⁻² bar⁻¹ for TFC-2. The rejection rate of salts and dyes of all the TFC membranes was better than the CA UF membrane. In particular, the TFC-2 membrane showed a desalination rate of up to 89%, and the rejection rate of malachite green and Congo red reached 89 and 85%, respectively. Such separation performance depends on the molecule’s concentration and pH of the feed solution. Overall, this study indicated that CHMA can serve as a potential candidate to produce TFC membranes for desalination and water treatment.

Declarations

Conflict of interest The authors confirm that there are no known conflicts of interest associated with this publication and there has been no significant financial support for this work that could have influenced its outcome.

References

- Sonawane GH, Shrivastava VS (2009) Kinetics of decolourization of malachite green from aqueous medium by maize cob (*Zea mays*): An agricultural solid waste. *Desalination* 247:430–441
- Makhetha TA, Moutloali RM (2018) Antifouling properties of Cu(tpa)@GO/PES composite membranes and selective dye rejection. *J Membr Sci* 554:195–210
- Guesmi Y, Agougui H, Lafi R, Jabli M, Hafiane A (2018) Synthesis of hydroxyapatite-sodium alginate via a co-precipitation technique for efficient adsorption of methylene blue dye. *J Mol Liq* 249:912–920
- Chai WS, Cheun JY, Kumar PS, Mubashir M, Majeed Z, Banat F, Ho S-H, Show PL (2021) A review on conventional and novel materials towards heavy metal adsorption in wastewater treatment application. *J Clean Prod* 296:126589
- Vlyssides AG, Papaioannou D, Loizidou M, Karlis KP, Zorpas AA (2000) Testing an electrochemical method for treatment of textile dye wastewater. *Waste Manag* 20:569–574
- Lim CL, Morad N, Teng TT, Norli I (2011) Chemical oxygen demand (COD) reduction of a reactive dye wastewater using H₂O₂/pyridine/Cu (II) system. *Desalination* 278:26–30
- Lee KM, Lai CW, Ngai KS, Juan JC (2016) Recent developments of zinc oxide based photocatalyst in water treatment technology: a review. *Water Res* 88:428–448
- Marrot B, Roche N (2002) Wastewater treatment and reuse in textile industries, a review. *Res Adv Water Res* 3:41–53
- Russo F, Castro-Muñoz R, Galiano F, Figoli A (2019) Unprecedented preparation of porous Matrimid (R) 5218 membranes. *J Membr Sci* 585:166–174
- Sotto A, Boromand A, Balta S, Kim J, Van der Bruggen B (2011) Doping of polyethersulfone nanofiltration membranes: antifouling effect observed at ultralow concentrations of TiO₂ nanoparticles. *J Mater Chem* 21:10311–10320
- Abdi G, Alizadeh A, Zinadini S, Moradi G (2018) Removal of dye and heavy metal ion using a novel synthetic polyethersulfone nanofiltration membrane modified by magnetic graphene oxide/metformin hybrid. *J Membr Sci* 552:326–335
- Al-Bastaki N (2004) Removal of methyl orange dye and Na₂SO₄ salt from synthetic waste water using reverse osmosis. *Chem Eng Process* 43:1561–1567
- Ursino C, Simone S, Donato L, Santoro S, De Santo MP, Drioli E, Di Nicolò E, Figoli A (2016) ECTFE membranes produced by non-toxic diluents for organic solvent filtration separation. *RSC Adv* 6:81001–810126
- White LS (2006) Development of large-scale applications in organic solvent nanofiltration and pervaporation for chemical and refining processes. *J Membr Sci* 286:26–35
- Cheng XQ, Zhang YL, Wang ZX, Guo ZH, Bai YP, Shao L (2014) Recent advances in polymeric solvent-resistant nanofiltration membrane. *Adv Polym Technol* 33:E1–E24
- Liu M, Chen Q, Lu K, Huang W, Lü Z, Zhou C, Gao C (2017) High efficient removal of dyes from aqueous solution through nanofiltration using diethanolamine-modified polyamide thin-film composite membrane. *Sep Purif Technol* 173:135–143
- Ghasemzadeh G, Momenpour M, Omidi F, Hosseini MR, Ahani M, Barzegari A (2014) Applications of nanomaterials in water treatment and environmental remediation. *Front Environ Sci Eng* 8:471–482
- Zhao FY, Ji YL, Weng XD, Mi YF, Ye CC, An QF, Gao C (2016) High-flux positively charged nanocomposite nanofiltration membranes filled with poly(dopamine) modified multiwall carbon nanotubes. *J ACS Appl Mater Interfaces* 8:6693–6700
- Song J, Li XM, Ursino C, Figoli A, He T (2016) membrane technologies for water treatment: removal of toxic trace elements with emphasis on arsenic fluoride and uranium. CRC Press, Taylor and Francis Group, Florida, pp 201–214
- Yuan F, Wang Z, Li S, Wang J, Wang S (2012) *J Membr Sci* 327:421–422
- Wu D, Huang Y, Yu S, Lawless D, Feng X (2014) Thin film composite nanofiltration membranes assembled layer-by-layer via interfacial polymerization from polyethylenimine and trimesoyl chloride. *J Membr Sci* 472:141–153
- Homayoonfal M, Akbari A, Mehrnia MR (2010) Preparation of polysulfone nanofiltration membranes by UV-assisted grafting polymerization for water softening. *Desalination* 263:217–225
- Abu Seman MN, Khayet M, Ali ZB, Hilal N (2010) Reduction of nanofiltration membrane fouling by UV-initiated graft polymerization technique. *J Membr Sci* 355:133–141
- Mah KH, Yusoff HW, Seman MA, Mohammad AW (2018) Polyester thin film composite nanofiltration membranes via interfacial polymerization: influence of five synthesis parameters on water permeability. *J Mech Eng Sci* 12:3387–3398
- Marquez JAD, Ang MBMY Jr, Doma BT, Huang SH, Tsai HA, Lee KR, Lai JY (2018) Application of cosolvent-assisted

- interfacial polymerization technique to fabricate thin-film composite polyamide pervaporation membranes with PVDF hollow fiber as support. *J Membr Sci* 564:722–731
26. Cadotte JE, Petersen RJ, Larson RE, Erickson EE (1980) A new thin-film composite seawater reverse osmosis membrane. *Desalination* 32:25–31
 27. J. E. Cadotte (1981) U.S. Patent No. 4,277,344. Washington, DC: U.S. Patent and Trademark Office.
 28. Bai L, Liu Y, Ding A, Ren N, Li G, Liang H (2019) Combined effects of PAC adsorption and in situ chlorination on membrane fouling in a pilot-scale coagulation and ultrafiltration process. *Chem Eng J* 358:1519–1528
 29. Meng J, Xie Y, Gu YH, Yan X, Chen Y, Guo XJ, Lang WZ (2021) PVDF-CaAlg nanofiltration membranes with dual thin-film-composite (TFC) structure and high permeation flux for dye removal. *Sep Purif Technol* 255:117739
 30. Zirehpour A, Rahimpour A, Ulbricht M (2017) Nano-sized metal organic framework to improve the structural properties and desalination performance of thin film composite forward osmosis membrane. *J Membr Sci* 531:59–67
 31. Wang X, Yeh TM, Wng Z, Yang R, Wang R, Ma H, Hsiao BS, Chu B (2014) Nanofiltration membranes prepared by interfacial polymerization on thin-film nanofibrous composite scaffold. *Polymer* 55:1358–1366
 32. Soroush A, Barzin J, Barikani M, Fathizadeh M (2012) Interfacially polymerized polyamide thin film composite membranes: preparation, characterization and performance evaluation. *Desalination* 287:310–316
 33. Cheng J, Shi W, Zhang L, Zhang R (2017) A novel polyester composite nanofiltration membrane formed by interfacial polymerization of pentaerythritol (PE) and trimesoyl chloride (TMC). *Appl Surf Sci* 416(416):152–159
 34. Wang L, Li D, Cheng L, Zhang L, Chen H (2013) Synthesis of 4-aminobenzoylpiperazine for preparing the thin film composite nanofiltration membrane by interfacial polymerization with TMC. *Sep Sci Technol* 48:466–472
 35. Mayhew TM, Burton GJ (1997) Stereology and its impact on our understanding of human placental functional morphology. *Microsc Res Techniq* 38:195–205
 36. Jusoh WZAW, Rahman SA, Ahmad AL, Mokhtar NM (2019) Fabrication and characterization of a polyamide thin-film composite membrane on a nylon 6,6 substrate for isopropanol dehydration. *C R Chim* 22:755–760
 37. Mohan DJ, Kullová L (2013) A study on the relationship between preparation condition and properties/performance of polyamide TFC membrane by IR DSC, TGA, and SEM techniques. *Desalin Water Treat* 51:586–596
 38. Ounifi I, Saidi N, Kahloul M, Sealey KS, Hafiane A, Ferjani E (2019) Synthesis and characterization of ultrafiltration membranes by phase inversion and by uropathogenic *Escherichia coli* retention performance. *Desalin Water Treat* 163:109–117
 39. Mubashir M, Dumée LF, Fong YY, Jusoh N, Lukose J, Chai WS, LokeShow P (2021) Cellulose acetate-based membranes by interfacial engineering and integration of ZIF-62 glass nanoparticles for CO₂ separation. *J Hazard Mater* 415:125639
 40. Mubashir M, Fong YY, Leng CT, Keong LK (2018) Enhanced gases separation of cellulose acetate membrane using N-methyl-1-2 pyrrolidone as fabrication solvent. *Int J Automot Mech Eng* 15(1):4978–4986
 41. Mubashir M, Fong YY, Leng CT, Keong LK (2019) Optimization of spinning parameters on the fabrication of NH₂-MIL-53(Al)/cellulose acetate (CA) hollow fiber mixed matrix membrane for CO₂ separation. *Sep Purif Technol* 215:32–43
 42. Ursino C, Di Nicolò E, Gabriele B, Criscuoli A, Figoli A (2019) Development of a novel perfluoropolyether (PFPE) hydrophobic/hydrophilic coated membranes for water treatment. *J Membr Sci* 581:58–71
 43. Castro-Muñoz R, Buera-Gonzalez J, de la Iglesia O, Galiano F, Fíla V, Malankowska M, Rubio C, Figoli A, Tellez C, Coronas J (2019) Towards the dehydration of ethanol using pervaporation cross-linked poly (vinyl alcohol)/graphene oxide membranes. *J Membr Sci* 582:423–434
 44. Xie W, Geise GM, Freeman BD, Lee HS, Byun G, McGrath JE (2012) Polyamide interfacial composite membranes prepared from m-phenylene diamine, trimesoyl chloride and a new disulfonated diamine. *J Membr Sci* 403:152–161
 45. Jenkins M, Tanner MB (1998) Operational experience with a new fouling resistant reverse osmosis membrane. *Desalination* 119:243–250
 46. Wei X, Kong X, Yang J, Zhang G, Chen J, Wang J (2013) Structure influence of hyperbranched polyester on structure and properties of synthesized nanofiltration membranes. *J Membr Sci* 440(440):67–67
 47. A. Figoli, S. Simone, E. Drioli (2015) Polymeric Membranes. In: CRC Press - Taylor & Francis Group (Ed.), *Membrane Fabrication*, London, United Kingdom. 28–69.
 48. Jo ES, An X, Ingole PG, Choi WK, Park YS, Lee HK (2017) CO₂/CH₄ separation using inside coated thin film composite hollow fiber membranes prepared by interfacial polymerization. *Chin J Chem Eng* 25:278–287
 49. Kushwaha OS, Avadhani C, Singh R (2014) Effect of UV rays on degradation and stability of high performance polymer membranes. *Adv Mater Lett* 5:272–279
 50. Ahmada A, Jamsheda F, Riaz T, Gul S, Waheed S, Sabir A, AlAnezif AA, Adrees M, Jamil T (2016) Self-sterilized composite membranes of cellulose acetate/polyethylene glycol for water desalination. *Carbohydr Polym* 149:207–216
 51. Talari ACS, Martinez MAG, Movasaghi Z, Rehman S, Rehman IU (2017) Advances in fourier transform infrared (FTIR) spectroscopy of biological tissues. *Appl Spectrosc Rev* 52:456–506
 52. Anan NSM, Jaafar J, Sato S, Mohamad R (2021) Titanium dioxide incorporated polyamide thin film composite photocatalytic membrane for bisphenol A removal. *IOP Conf Ser Mater Sci Eng* 1142:012015
 53. Tang CYY, Kwon YN, Leckie JO (2009) Effect of membrane chemistry and coating layer on physicochemical properties of thin film composite polyamide RO and NF membranes II. Membrane physicochemical properties and their dependence on polyamide and coating layers. *Desalination* 242:168–182
 54. Ounifi I, Guesmi Y, Ursino C, Santoro S, Mahfoudhi S, Figoli A, Ferjanie E, Hafiane A (2021) Antifouling membranes based on cellulose acetate (CA) blended with poly(acrylic acid) for heavy metal remediation. *Appl Sci* 11:4354
 55. Roh IJ, Greenberg AR, Khare VP (2006) Synthesis and characterization of interfacially polymerized polyamide thin films. *Desalination* 191:279–290
 56. Song Y, Sun P, Henry LL, Sun B (2005) Mechanisms of structure and performance controlled thin film composite membrane formation via interfacial polymerization process. *J Membr Sci* 251:67–79
 57. Ingole PG, Choi WK, Baek IH, Lee HK (2015) Highly selective thin film composite hollow fiber membranes for mixed vapor/gas separation. *RSC Adv* 5:78950–78957
 58. Wei J, Liu X, Qiu C, Wang R, Tang CY (2011) Influence of monomer concentrations on the performance of polyamide-based thin-film composite forward osmosis membranes. *J Membr Sci* 381:110–117
 59. Hamad H, Bassyouni D, El-Ashtouky ES, Amin N, El-Latif MA (2018) Electrocatalytic degradation and minimization of specific energy consumption of synthetic azo dye from wastewater by anodic oxidation process with an emphasis on enhancing

- economic efficiency and reaction mechanism. *Ecotoxicol Environ Saf* 148:501–512
60. Bai L, Liu Y, Ding A, Ren N, Li G, Liang H (2019) Fabrication and characterization of thin-film composite (TFC) nanofiltration membranes incorporated with cellulose nanocrystals (CNCs) for enhanced desalination performance and dye removal. *Chem Eng J* 358:1519–1528
61. Mousavi SR, Asghari M, Mahmoodi NM (2020) Chitosan-wrapped multiwalled carbon nanotube as filler within PEBA thin film nanocomposite (TFN) membrane to improve dye removal. *Carbohydr Polym* 237:116128
62. Wei X, Wang S, Shi Y, Xiang H, Chen J (2014) Application of positively charged composite hollow-fiber nanofiltration membranes for dye purification. *Ind Eng Chem Res* 53:14036–14045

Publisher's Note Springer Nature remains neutral with regard to jurisdictional claims in published maps and institutional affiliations.